PROCEEDINGS of the
23rd International Congress on Acoustics

9 to 13 September 2019 in Aachen, Germany

Parametric Study of the Estimation of Indoor Trolley Wheel Stiffness for Use in a Rolling Noise Prediction Model

Matt EDWARDS[1]; Fabien CHEVILLOTTE[2]; François-Xavier BÉCOT[3]; Luc JAOUEN[4]; Nicolas TOTARO[5]

[1-4] Matelys – Research Lab, France

[5] Univ Lyon, INSA-Lyon, Laboratoire Vibrations Acoustique, France

ABSTRACT

In vehicle tyre/road contact modelling, dynamic models are typically used which incorporate the vehicle's suspension in their estimation: thus relying on a known stiffness to determine the movement of the wheel in response to roughness excitation. For the case of a wheeled device rolling on a floor (such as a delivery trolley moving merchandise inside a commercial building), there is often no suspension, yet the wheel is still too soft to able to be considered mechanically rigid. An indoor rolling prediction model needs to provide a robust way of estimating the wheel's effective stiffness. This work presents an original technique for estimating the stiffness of an indoor cylindrical trolley wheel. A parametric study was conducted in order to identify the dependence of the wheel stiffness on each of the relevant variables: including the wheel's radius, axle size, width, applied load, and material properties. The methodology may be used to estimate the stiffness of new wheel types (i.e. different geometries and materials) without needing to solve a finite element model each time.

Keywords: Wheel, Stiffness, Prediction

1. INTRODUCTION

In the world of acoustics, prediction models that estimate the sound produced in a rolling event are widespread. Mostly existing for automotive tyre/road (1–3) and train wheel/rail contact (4–6), these models calculate the interaction forces between the two bodies (the wheel and the surface upon which the wheel rolls), which are produced by the small-scale relative roughness in the contact area (7,8). These forces induce motion in the two bodies, and their resulting structural vibration is what radiates sound to the surrounding area. Recently, work has been done to develop a prediction model applicable to indoor rolling scenarios as well, such as that of a delivery trolley rolling on a floor inside a commercial space (9).

For such a model, it is necessary to know the stiffness of the wheels of the trolley in order to accurately estimate their dynamic motion for calculating their radiated sound emission. For a vehicle with a built-in suspension system, the stiffness is straightforward to calculate: it is simply the stiffness of the suspension spring. However, most trolleys do not have suspension systems: they are purely made up of a wheel turning about a rigid axle. In such a scenario, the stiffness used is instead the stiffness of the wheel itself. Considering the vast range of sizes and materials that trolley wheels come in, this presents a challenge for incorporation into a sound prediction model that wishes to be widely applicable for a range of indoor rolling scenarios.

One option may be to build a finite element (FE) model for a given wheel, but this is costly, as it requires a new FE model to be run for every single unique geometry/material composition. An alternative option would be to run a series of FE models in the form of a parametric study, extract trends in the data, and develop a system for estimating the stiffness of any geometry or material

[1] matthew.edwards@matelys.com
[2] fabien.chevillotte@matelys.com
[3] francois-xavier.becot@matelys.com
[4] luc.jaouen@matelys.com
[5] nicolas.totaro@insa-lyon.fr

composition, without the need to solve a new FE model each time. In this paper, a straightforward method is proposed to characterize the compressional stiffness of a cylindrical wheel in contact with a flat surface. This is inspired by the methodology used by Sim and Kim to estimate the elastic properties of viscoelastic materials (10). A two-dimensional surface plot is derived from high order FE models of a cylindrical wheel under static vertical compression, linking the wheel/axle radii ratio and contact area half-length. This forms an abacus which may be referenced to find a given wheel's stiffness. Such an abacus may be incorporated into an indoor rolling noise prediction model: allowing for a more precise estimation of the movement of the wheel and leading to increased accuracy in sound predictions.

2. PARAMETRIC STUDY

In order to identify what kind of an influence each of the various wheel parameters had on its stiffness, a parametric study was conducted. A series of FE models were run for cylindrical wheels of various geometries and material compositions, from which trends were identified. For the parametric study, four geometric variables, shown in Figure 1, were chosen to be investigated: wheel radius r_W, axle radius r_A, wheel width w, and contact area half-length a. Additionally, Young's modulus E and Poisson's ratio ν of the wheel material, as well as the input displacement z_{in}, were also included.

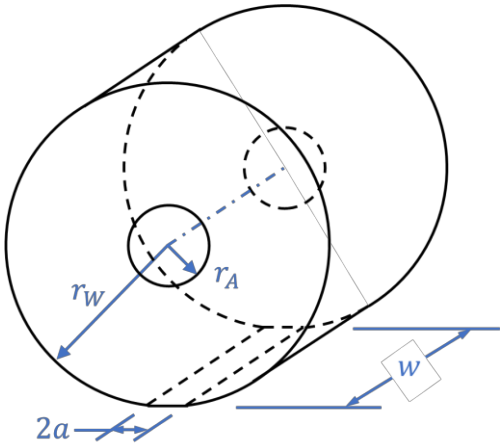

Figure 1 – Description of the wheel geometry.

2.1. Meshing

The mesh densities of the FE models were first defined based on the width of the wheel, having a maximum edge length of $w/7$. They were then re-meshed to add extra nodes in the area of contact for particularly small contact area half-lengths. This ensured the contact area had at least 4 nodes along its length. Depending on the geometry, mesh sizes ranged between $1.0 \cdot 10^4$ and $5.3 \cdot 10^4$ nodes, having degrees of freedom between $2.1 \cdot 10^6$ and $1.1 \cdot 10^7$.

To solve the FE model, the flat contact surface on the bottom of the wheel was fixed in place. A uniform displacement in the downward vertical direction was imposed on the axle surface, simulating the mass of the trolley borne by the wheel under load. A glued condition between the axle and wheel was assumed for the purpose of FE calculations. The stiffness of each FE model was calculated by integrating the vertical normal stress and vertical displacement across all the nodes on the axle surface, then dividing the two.

2.2. Comparison with an Equivalent Beam

The stiffness of a beam in axial compression is given by

$$K_{\text{beam}} = \frac{AE}{L} \tag{1}$$

where A and L are the cross-sectional area and height of the beam, respectively. If the wheel is represented as a beam with cross-section equal to the contact area and height equal to the distance between the contact area and the bottom of the axle, then Equation 1 may be rewritten as

$$K_{\text{beam}} = \frac{2awE}{\sqrt{{r_W}^2 - a^2} - r_A} \tag{2}$$

which may be used as comparison with the results of the parametric study to see how the two differ in application.

2.3. Influence of Parameters

Figure 2 shows the results of the FE simulations, which revealed patterns in how the wheel stiffness is influenced by each of the various parameters: some expected, some not. Each plot shows the influence of a single parameter, displayed along the horizontal axis. Each plot also shows results for multiple values of Poisson's ratio (0-0.495). The parameters having a linear influence on the wheel stiffness are Young's modulus and the wheel width. For a given FE model, a change in either of these values results in a proportional change to the wheel stiffness. Since Young's modulus of a material is essentially a measure of that material's intrinsic stiffness independent of shape, logic follows that it would be linearly proportional to the actual wheel stiffness. Similarly, increasing the width of the wheel essentially acts like adding springs in parallel, thus increasing the stiffness in a linear fashion. Both of these parameters act identically as they do in Equation 2 for the equivalent beam.

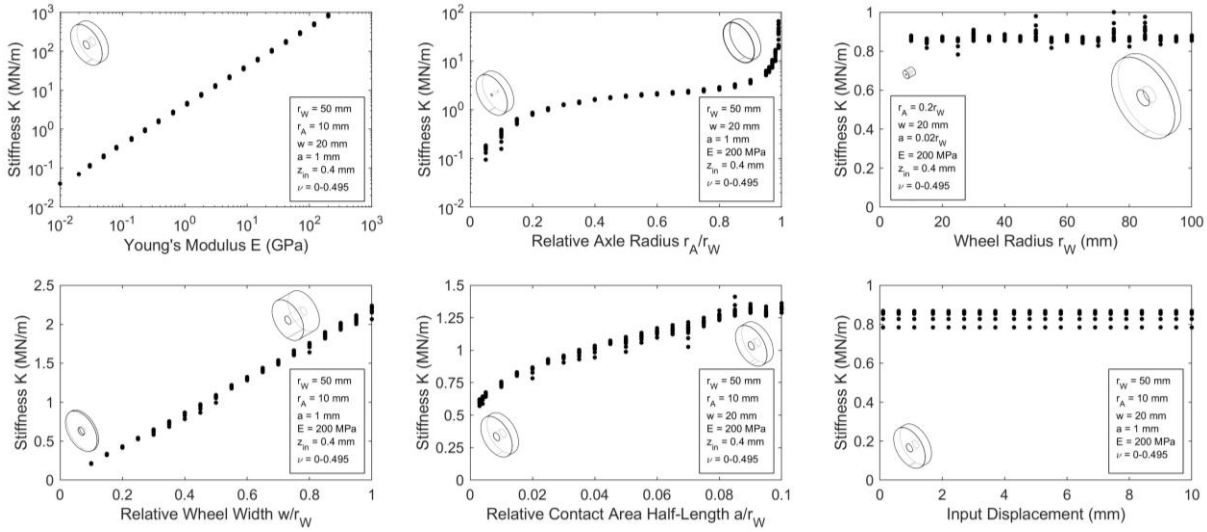

Figure 2 – Results of the Parametric Study. From left to right, top to bottom: Young's Modulus E, relative axle radius r_A/r_W, wheel radius r_W, relative wheel width w/r_W, relative contact area half-length a/r_W, and input displacement z_{in}. Points having the same x coordinate (but a different y coordinate) are for varying values for Poisson's ratio ν. Schematics of the extreme wheel geometries on each plot are shown for reference (drawn to scale with respect to one another).

The two parameters exhibiting unique relationships with the wheel stiffness are the axle radius and the contact area half-length. Neither may be described by a simple expression, and will thus become the topic of further investigation in section 3. For the axle radius: as the ratio between the axle radius and the wheel radius approaches unity, the stiffness approaches infinity. Since the axle is considered rigid in the FE models, as the volume of wheel material approaches zero, the compressed wheel gets closer and closer to exhibiting that of a rigid connection, thus having infinite stiffness. For the contact area half-length: as the size of the contact area approaches zero, the stiffness begins to drop off exponentially. Due to limitations with the meshing software, extremely small values for the contact area half-length (below 0.3% of the wheel radius) were not able to be reliably meshed.

Finally, there are three parameters which have little or no influence on the wheel stiffness: the wheel radius, input displacement, and Poisson's ratio. The first comes with a caveat, as the ratio between the axle radius and the wheel radius does indeed have a strong effect on the wheel stiffness. However, when this ratio is held constant, increasing the wheel radius does not result in any change in wheel stiffness. So perhaps it is better to say that the wheel radius *does* have an effect on the stiffness, but that this effect can be fully described by the changing axle/wheel radii ratio. In regards

to input displacement, the lack of dependence is in accordance with the use of a linear material in the FE models, where increasing compression does not result in increased stiffness.

The lack of dependence on Poisson's ratio was unexpected, as an elastic solid of uniform cylindrical or rectangular prism shape, compressed in the axial direction, is known to have a high dependency on Poisson's ratio (10). Looking across all six plots in Figure 2, a change in Poison's ratio resulted in essentially no change in stiffness (all else held constant). The points which exhibit the largest deviation are all for the highest values of Poisson's ratio (above 0.49), and they do not occur in a consistent fashion (i.e. not always an increase and not always a decrease). In essence, the stiffness is remaining nearly unchanged for all values of Poisson's ratio all the way up until around 0.49, where only then the modelling instability that exists when approaching $\nu = 0.5$ starts to have a minor effect. When loaded in the vertical direction, it is the effect of the wheel shape which dominates. The cylindrical form allows the wheel material to "move out of the way" under compression into the horn-shaped free space between the wheel and the floor. The shape of the geometry itself is linking the movement of the two transverse directions to that of the longitudinal direction in a way that negates any influence that the Poisson effect may have.

3. GENERATION OF THE ABACUS

To generate the abacus, a second series of FE models were run for the two chosen nonlinearly dependent variables: the axle radius and the contact area half-length: both normalized by the wheel radius. Eighteen values between 0.05 and 0.98 were chosen for the axle/wheel radii ratio r_A/r_W. Eighteen values between 0.003 and 0.1 were chosen for the relative contact area half-length a/r_W. Constant values of $w/r_W = 0.4$, $E = 1$ Pa, $\nu = 0.3$, and $z_{in} = 0.1$ mm were chosen for the wheel width, Young's modulus, and Poisson's ratio, respectively. Though it should be noted that, due to their relationship with the wheel stiffness (linear for w and E, and independent for υ and z_{in}), their choice is arbitrary.

3.1. Normalized wheel stiffness

Figure 3 shows the results of the second series of FE calculations. Equation 3 is first used to find the normalized wheel stiffness by dividing by Young's modulus and the wheel width

$$K_{\text{norm}} = \frac{K}{wE} \tag{3}$$

The normalized stiffness is then plotted as a function of the axle/wheel radii ratio and relative contact area half-length. A two-dimensional linearly interpolated surface is overlaid to connect the data points. The data is plotted with a logarithmic z-scale (base 10) in order to visualize how the stiffness changes for both low and high values of r_A/r_W. As the axle/wheel radii ratio grows, so does the influence of the size of the contact area on the stiffness. For ratios 0-0.8, there is a 1.5x factor in the change in normalized stiffness. Above 0.8 the stiffness increases exponentially, up to a factor of nearly 16x. Figure 3 may be used as an abacus, allowing one to find the normalized wheel stiffness for a cylindrical wheel of any reasonable size (i.e. for $0.05 \leq r_A/r_W \leq 1$ and $0.003 \leq a/r_W \leq 0.1$). This encompasses nearly every type of cylindrical solid wheel which would be expected to be found on an indoor trolley. This procedure may be implemented into an indoor rolling noise prediction model to provide an accurate estimation of the wheel stiffness.

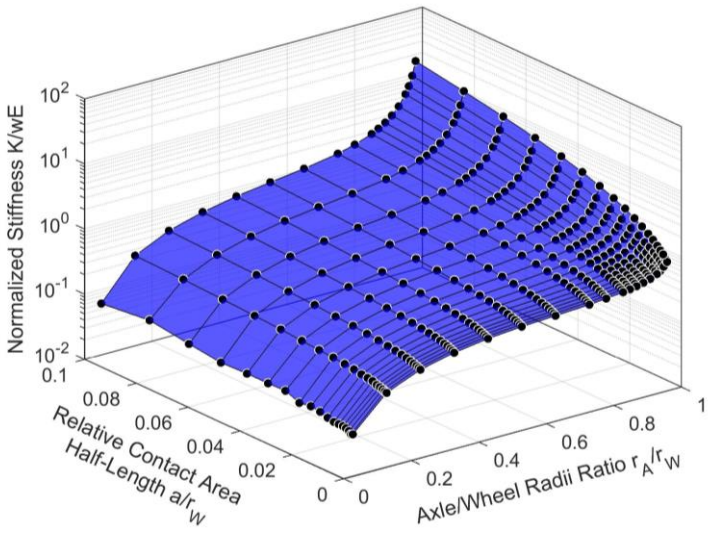

Figure 3 – Normalized wheel stiffness as a function of axle/wheel radii ratio and relative contact area half-length (black points). A two-dimensional linearly-interpolated surface (shown in blue) has been overlaid to form the abacus. Plotted on a logarithmic z-scale (base 10).

3.2. Example Estimation

The process of using the abacus is relatively straightforward. As an example, let us take a wheel with the following properties: $E = 200$ MPa, $\nu = 0.3$, $r_W = 60$ mm, $r_A = 5$ mm, $w = 35$ mm. For a cylindrical wheel, Hertzian contact theory states the size of the contact area to be

$$a = \sqrt{\frac{4Qr_W}{\pi w E^*}} \tag{4}$$

where Q is the applied load, and E^* is the apparent Young's Modulus between the wheel and floor

$$E^* = \left(\frac{1 - \nu_{wheel}{}^2}{E_{wheel}} + \frac{1 - \nu_{floor}{}^2}{E_{floor}} \right)^{-1} \tag{5}$$

For the example, we will use a concrete floor ($E = 3.3$ GPa, $\nu = 0.2$). If the wheel is put under a static load of $Q = 200$ N, Equations 3-4 estimate a contact area half-length of $a = 1.45$ mm. Plugging these values into the abacus presented in section 3.1, we estimate a normalized wheel stiffness of $K_{norm} = 0.087$. Finally, using Equation 3, we obtain a wheel stiffness of $K = 607$ kN/m.

4. SCOPE OF THE METHOD'S APPLICABILITY

In development of both the parametric study and the abacus, care was taken to run FE models for a wide range of parameter values. Thus, for the most part, any kind of trolley wheel which may be reasonably expected to be found in the real world can have this method applied. Due to their linear dependence, for the wheel width, radius, and Young's modulus, any value may be used. Axle radii of 5-98% of the wheel radius are valid, which for all intents and purposes is comprehensive, as a wheel outside this range would be of no practical use. For the contact area half-length, the method is assumed to be valid for any value below 10% of the wheel radius. Again, the wheel softness and applied load would need to be so high to achieve a contact area half-length above this limit, that in reality it is of no concern. For values below 0.3% of the wheel radius, the wheel stiffness is assumed to continue to follow the linear profile extrapolated from between the values at $0.003r_W$ and $0.0036r_W$. This results in an overestimation of the stiffness for these extremely small contact area half-lengths. However, this is considered acceptable in order to allow the model to allow for loss of contact between the wheel and the floor: a possibility in the presence of wheel flats and/or floor joints. In this type of situation, the size of the contact area tends to zero before disappearing at the moment of loss of contact.

On a larger scale, the results show in this paper (particularly in regards to the discovery of the lack of influence of the Poisson effect) demonstrate that a similar modeling technique may be used to

characterize the properties of other shapes as well. Characterizations have been performed for constant circular cross sections (10,11) (for which the Poisson effect plays a large role), and characterizations of materials with constant square cross sections yield results which are nearly identical to those of a constant circular cross section below Poisson's ratios of about 0.47. However, analysis of other non-constant cross sections, or even more complex shapes, could potentially provide beneficial insights in applications and industries beyond rolling contact modeling.

In a future work, it will be shown how the abacus may be used to derive polynomial relationships between the stiffness, axle/wheel radii ratio, and relative contact area half-length. It is possible for either a single two-dimensional expression or a series of one-dimensional expressions to be developed to fully characterize the wheel stiffness. This eliminates the need for interpolation, leading to increased accuracy and applicability in the estimation technique.

5. CONCLUSIONS

This work presents an original technique for estimating the stiffness of a cylindrical trolley wheel. A parametric study was conducted to identify the dependence of the wheel stiffness on each of the relevant variables. The stiffness is linearly dependent on the wheel width and Young's modulus, and largely independent from Poisson's ratio. A unique dependency exists for the axle/wheel radii ratio and contact area half-length. Using the information from these relationships, an abacus was created by generating a two-dimensional linearly interpolated surface for estimating the stiffness of virtually any cylindrical wheel. The abacus and can be implemented into a rolling noise model to provide an accurate estimation of the wheel stiffness. In a future work, it will be shown how the abacus may be replaced by one or two-dimensional polynomial relations to further improve the estimation process.

ACKNOWLEDGEMENTS

The work was done as part of Acoutect: an innovative training network composed of 5 academic and 7 non-academic participants. This consortium comprises various disciplines and sectors within building acoustics and beyond, promoting intersectoral, interdisciplinary and innovative training and mobility of the researchers within the project. This project has received funding from the European Union's Horizon 2020 research and innovation programme under grant agreement No 721536.

REFERENCES

1. Clapp TG, Eberhardt AC, Kelley CT. Development and Validation of a Method for Approximating Road Surface Texture-Induced Contact Pressure in Tire-Pavement Interaction. Tire Science and Technology. 1988;16(1):2–17.
2. Wullens F, Kropp W. A Three-Dimensional Contact Model for Tyre/Road Interaction in Rolling Conditions. Acta Acustica United with Acustica. 2004;90:702–11.
3. Rustighi E, Elliott SJ. Stochastic Road Excitation and Control Feasibility in a 2D Linear Tyre Model. Journal of Sound and Vibration. 2007;300(3):490–501.
4. Thompson DJ, Hemsworth B, Vincent N. Experimental Validation of the TWINS Prediction Program for Rolling Noise, Part 1: Description of the Model and Method. Journal of Sound and Vibration. 1996;193(1):123–35.
5. Thompson DJ, Fodiman P, Mahé H. Experimental Validation of the TWINS Prediction Program for Rolling Noise, Part 2: Results. Journal of Sound and Vibration. 1996;193(1):137–47.
6. Pieringer A, Kropp W, Thompson DJ. Investigation of the Dynamic Contact Filter Effect in Vertical Wheel/Rail Interaction using a 2D and a 3D Non-Hertzian Contact Model. Wear. 2011;271(1):328–38.
7. Remington PJ. Wheel/Rail Rolling Noise: What do we know? What don't we know? Where do we go from here? Journal of Sound and Vibration. 1988;120(2):203–26.
8. Kuijpers A, Blokland G. Tyre/Road Noise Models in the Last two Decades: A Critical Evaluation. In The Hague, Holland; 2001.
9. Edwards M, Chevillotte F, Jaouen L, Bécot F-X, Totaro N. Rolling Noise Modeling in Buildings. In Chicago, IL USA; 2018.
10. Sim S, Kim K-J. A method to determine the complex modulus and poisson's ratio of viscoelastic materials for FEM applications. Journal of Sound and Vibration. 1990;141(1):71–82.
11. ISO 18437-5:2011 - Mechanical vibration and shock -- Characterization of the dynamic mechanical properties of visco-elastic materials -- Part 5: Poisson ratio based on comparison between measurements and finite element analysis.